Available online at www.sciencedirect.com
ScienceDirect
Trans. Nonferrous Met. Soc. China 22(2012) 2351−2356
Transactions of Nonferrous Metals Society of China
www.tnmsc.cn

Mechanical properties of Mg−6Gd−1Y−0.5Zr alloy processed by low temperature thermo-mechanical treatment

LI De-jiang[1], ZENG Xiao-qin[1], XIE Yan-cai[1], WU Yu-juan[1], DING Wen-jiang[1], CHEN Bin[2]

1. State Key Laboratory of Metal Matrix Composites, School of Materials Science and Engineering, Shanghai Jiao Tong University, Shanghai 200240, China;
2. Instrumental Analysis Center of School of Materials Science and Engineering, Shanghai Jiao Tong University, Shanghai 200240, China

Received 9 July 2012; accepted 24 August 2012

Abstract: An as-solution treated Mg−6Gd−1Y−0.4Zr alloy was processed by low temperature thermo-mechanical treatments (LT-TMT), including cold tension with various strains followed by aging at 200 °C to peak hardness. The results show that the precipitation kinetics of the alloy experienced LT-TMT is greatly accelerated and the aging time to peak hardness is greatly decreased with increasing tensile strain. The tensile yield strength, ultimate tensile strength and elongation at room temperature of the alloy after cold tension with strain of 10% and peak aging at 200 °C are 251 MPa, 296 MPa and 8%, respectively, which are superior to the commercial heat-resistant WE54 alloy, although the latter has a higher rare earth element content.

Key words: Mg−Gd−Y−Zr alloy; low temperature thermo-mechanical treatment; precipitation hardening; mechanical properties

1 Introduction

Precipitation hardening magnesium (Mg) alloys containing rare earth (RE) elements are attractive in aerospace and racing automotive industries for their high specific strength and excellent thermal stability at elevated temperatures [1]. The good performances of these alloys are attributed to the decomposition of series metastable phases which are completely coherent or semi-coherent with the matrix during aging treatment [2−5]. The precipitation sequence and mechanical properties of such alloy systems have been studied by some researchers [6−8]. Generally, a four stages precipitation sequence involving S.S.S.S.(HCP)→$\beta''(D0_{19})$→β'(CBCO)→β_1(FCC)→β(FCC) has been suggested and the metastable β' and β_1 phases are contributed to the peak hardness.

It is well known that the mechanical properties of age-hardenable aluminum alloys could be markedly improved by proper application of thermo-mechanical treatments (TMT), which relies on a combination of plastic deformation and aging treatment [9,10]. It has been demonstrated that cold work (6% or 10% deformation strain by cold rolling) prior to aging could introduce high density of twins and dislocations and promote the precipitation in WE54 alloy [11]. However, technologies especially low temperature TMT (LT-TMT) have not been yet carried out on the prominent age hardenable Mg−Gd−Y(−Zr) series alloys.

The present study is to evaluate the effects of LT-TMT, involving cold tension with various strains followed by artificial aging to peak hardness, on the precipitation process and mechanical properties of the Mg−6Gd−1Y−0.4Zr (GW61K) alloy, and then the mechanical properties were compared with those of the commercial WE43 alloy, since both GW61K and WE43 alloys have the same total RE elements content of 7%.

2 Experimental

The as-cast Mg−6Gd−1Y−0.4Zr (mass fraction, %) alloy specimens were solution-treated at 500 °C for 6 h, followed by quenching in hot water at temperature of

Foundation item: Projects (50971089, 51171113, 51001072) supported by the National Natural Science Foundation of China; Projects (2012M511089, 20090460615, 201003267) supported by the Postdoctoral Science Foundation of China
Corresponding author: WU Yu-juan, Tel: +86-21-54742627, Fax: +86-21-34202794; E-mail: wuyj@sjtu.edu.cn
DOI: 10.1016/S1003-6326(11)61470-2

80 °C. The as-solution treated specimens were machined and cold tensioned at a strain rate of 6.7×10^{-4} s^{-1} and strains of 0, 5%, 10% and 20%, respectively, and then isothermally aged at 200 °C. The process of the Mg solid solution decomposition during aging was checked by hardness measurement. The Vickers-hardness was measured under a 49 N load for 30 s. The tensile specimens were tested at room temperature on a Zwick/Roell testing machine at a strain rate of 1.67×10^{-3} s^{-1}. The characterization of phases and metallographic sections perpendicular to the ruptured surface was performed by optical microscope (OM, LEICA MEF4M) and transmission electron microscope (TEM, JEOL 2010 operated at 200 kV), respectively. Thin foils for TEM observation were prepared according to a standard twin-jet electro-polishing. The ruptured surfaces were examined by scanning electron microscopy (SEM, JEOL SEM6490).

3 Results and discussion

3.1 Microstructure after cold tension

Figure 1 shows the optical microstructures of the as-solution treated GW61K alloy and after cold tension with various strains. After solution treatment, the grains of the alloy are equiaxed and the average grain size is 40−50 μm (Fig. 1(a)). It could be also found that a number of block-shaped particles has formed during solution treatment which are distributed at grain boundaries and inner grains. Figure 2 shows the TEM micrograph and SAED pattern of the block-shaped phase in the as-solution treated GW61K alloy. As shown

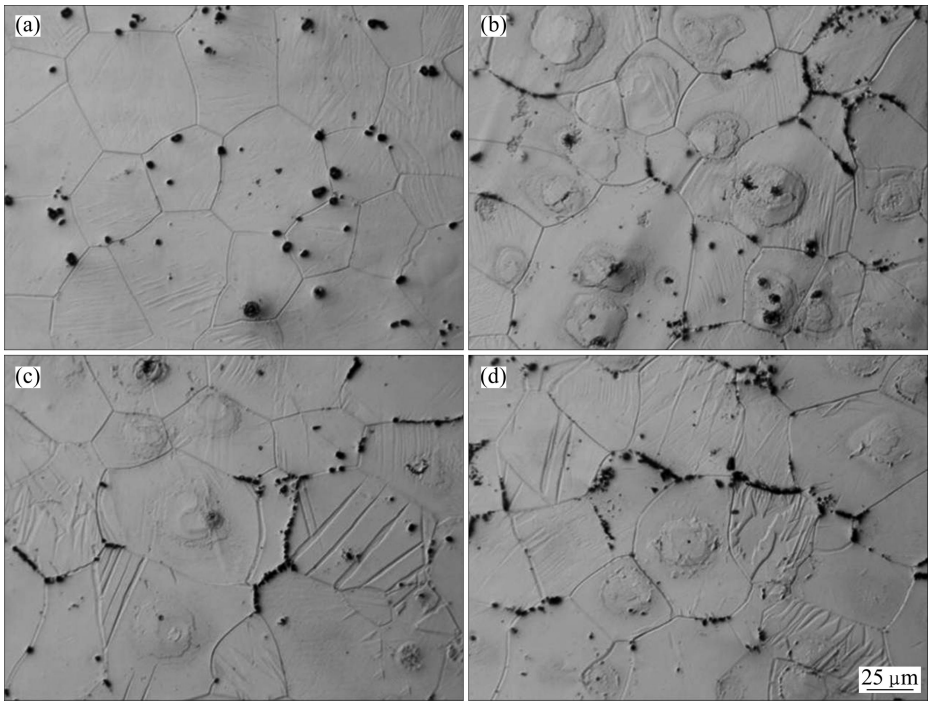

Fig. 1 Optical microstructures of as-solution treated GW61K alloy and after cold tension with various strains: (a) As-solution treated; (b) Strain of 5%; (c) Strain of 10%; (d) Strain of 20%

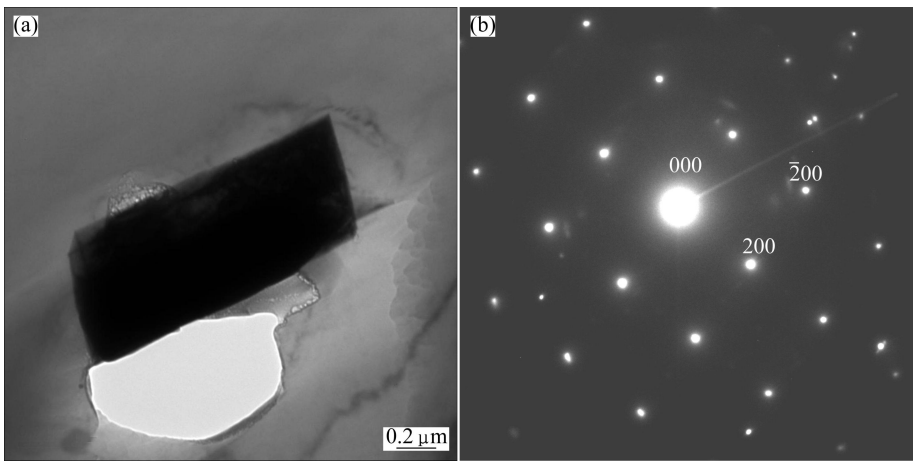

Fig. 2 TEM image (a) and SAED pattern (b) of block-shaped phase in as-solution treated GW61K alloy

in Fig. 2(a), the particles are distinctly observed block-shaped. Moreover, as shown in Fig. 2(b), the SAED pattern is confirmed that this block-shaped phase has FCC crystal structure (a≈0.56 nm), which is coincident with the results studied by HE et al [7] in Mg−10Gd−3Y−0.5Zr alloy. The EDS result in TEM mode investigated for the phase is RE-enrichment, but the inherent stoichiometric composition remains unclear.

It is seen that there are no evident differences in the microstructures of the alloy specimens after cold tension with various strains (Figs. 1(b)−(d)) from that of the as-solution treated alloy (Fig. 1(a)), except deformation twins in some grains. As can be seen in Fig. 1, the amount of twins increases with increasing strain, however, the total number of twins in the alloys is less than that in the Mg−Al−Zn and Mg−Al−Mn alloys [12,13] after cold deformation with almost the same strain. For example, very few amounts of twins could be observed in the alloy after cold tension with strain of 10% (Fig. 1(c)), indicating that the strain is contributed mainly by dislocation slipping. According to some studies [13,14], most of the twins should be identified as $\{10\bar{1}2\}\langle 10\bar{1}1\rangle$ twin system.

3.2 Age hardening characteristics

Figure 3 shows the Vickers hardness as a function of aging time at 200 °C in the GW61K alloys after cold tension with various strains. The initial hardness increases with increasing strain of cold tension due to strain hardening. For example, the hardness for the alloy after cold tension with strain of 10% is HV 61.8, which is 23.1% higher than that of the as-solution treated alloy of HV 50.2. During aging treatment, the hardening curve of the as-solution treated alloy (no strain) shows a typical three-stage, which are under-aging stage, peak-aging stage and over-aging stage.

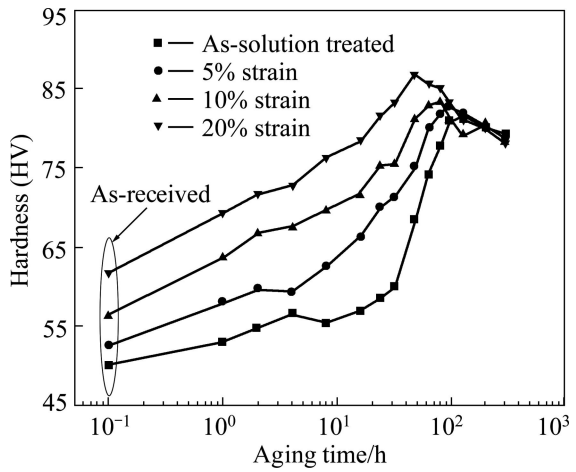

Fig. 3 Vickers hardness as function of aging time at 200 °C in GW61K alloys after cold tension with various strains

HE et al [15] explained that the typical three-stage should be attributed to the formation of three different metastable phases during corresponding stages in the Mg−Gd−Y−Zr alloy such as an Mg−10Gd−2Y−0.5Zr alloy. At the first stage, the formation of β'' phase makes the hardness show a steady increasing trend; at the second stage, a great number of β' phases come into being which makes the hardness increase rapidly until a peak value of HV 81.7 at 200 °C for 128 h could be reached and even still exists in over-aging stage; then the hardness decreases gradually for the reason of transformation from β' phase to β_1 and β phases at the third stage.

For the deformed GW61K alloys, the aging time to peak hardness decreases greatly with increasing the the deformation strain, as seen in Fig. 3. The peak aging time is 128, 96, 80 and 48 h, and the corresponding peak Vickers hardness values are HV 81.7, 82.8, 83.6 and 86.8 after cold deformation with strains of 0, 5%, 10% and 20%, respectively. However, the second stage (rapidly increasing) seems to be absent in the age hardening curves, for example, a three-stage still can be observed for the alloys after cold deformation with strain of 5%, while, only two-stage remains for the alloys after cold deformation with strains of 10% and 20%. This should be possibly attributed to the precipitation involving β' phase rather than β'' phase from the deformed alloys during ageing treatment at the early stage, which also indicates that cold deformation prior to aging can accelerate the precipitation kinetics of β' phase effectively. Figure 4 shows the TEM image and SAED pattern taken from the $[0001]_{Mg}$ of the precipitates in the alloy after cold deformation with strain of 10% and aging at 200 °C for 36 h, which is coincident with β' phase observed in an Mg−10Gd−3Y−0.5Zr alloy [7].

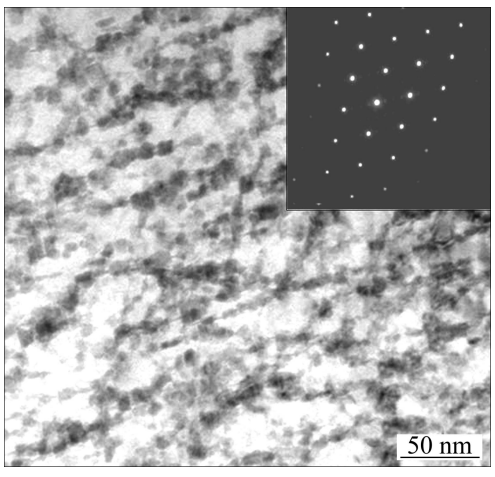

Fig. 4 TEM image and SAED pattern showing precipitates in alloy after cold tension with strain of 10% and aging at 200 °C for 36 h

3.3 Mechanical properties

Table 1 lists the tensile properties at room temperature of the age-treated GW61K alloys after LT-TMT at cold tension with various strains of 0, 5%, 10% and 20%, respectively, together with commercial WE43 and WE54 alloys. It can be seen that the tensile yield strength and ultimate tensile strength of the LT-TMTed GW61K alloys increase with increasing cold deformation strain, while the elongation decreases. The optimum combination of strength and ductility could be obtained in the alloy after cold deformation with strain of 10% and aging at 200 °C for 36 h. The tensile yield strength, ultimate tensile strength and elongation are 251 MPa, 296 MPa and 8%, respectively, which are superior to those of WE43 and WE54 alloys, although the studied GW61K alloy has a lower total RE elements content than that of WE54 alloy. It also implies that LT-TMT should be an effective way to further improve the mechanical properties of Mg−RE series alloys.

Table 1 Tensile properties at room temperature of age-treated GW61K alloys after LT-TMT at cold tension with various strains, commercial WE43 and WE54 alloys

Aging-treated alloys	Tensile yield strength/MPa	Ultimate tensile strength/MPa	Elongation/ %
GW61K, 0 strain,T6	160	273	20
GW61K,T4, 5% strain, T5	213	290	13
GW61K, T4, 10% strain, T5	251	296	8
GW61K,T4, 20% strain, T5	268	314	3.5
WE43, T6 [16]	180	250	7
WE54, T6 [17]	205	280	4

T6 for as-solution treated GW61K: 500 °C for 6 h +200 °C for 128 h; T4 for GW61K with 5% strain 500 °C for 6 h; T5 for GW61K with 5% strain: 200 °C for 96 h; T5 for GW61K with 10% strain: 200 °C for 80 h; T5 for GW61K with 20% strain: 200 °C for 80 h.

Figures 5 and 6 show the optical images of the rupture samples adjacent to the fracture surface and SEM images perpendicular to the fracture surface of GW61K alloy T6-treated, LT-TMTed with 10% cold deformation and then aged at 200 °C for 80 h. As seen in Fig. 5(a), most of the cracks are observed along grain boundaries in the T6-treated alloy, which indicates that the cracks should initiate from grain boundaries especially triangular grain boundaries.

The fracture micrograph in the T6-treated alloy shows quasi-cleavage fracture mechanism [18] with the existence of cleavage planes and large amounts of tear ridges and dimples, as shown in Fig. 5(b), which is consistent with the good ductility (about 20%) of the alloy under such condition. Figure 6(a) shows the cracks located mainly in grain interiors along twin boundaries in the LT-TMTed alloy, trans-granular fracture pattern could

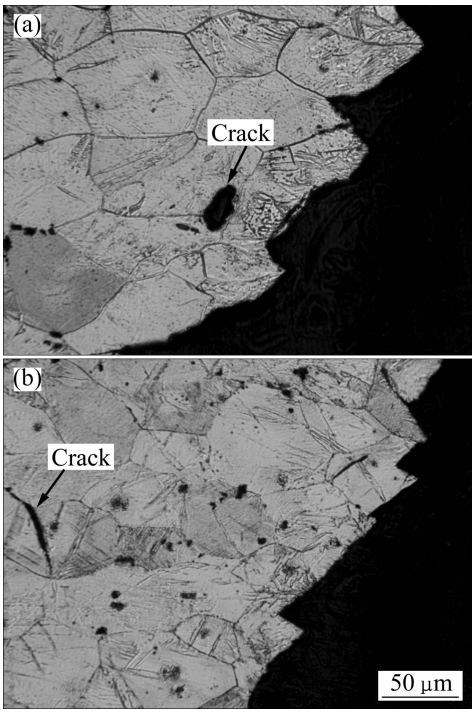

Fig. 5 Optical images of rupture samples adjacent to fracture surface of GW61K alloy: (a) T6-treated; (b) LT-TMTed with 10% cold deformation and then aged at 200 °C for 80 h

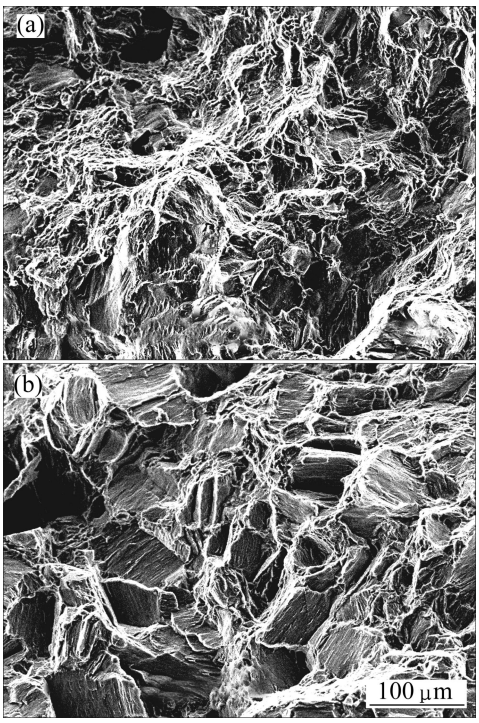

Fig. 6 SEM images perpendicular to fracture surface of GW61K alloy: (a) T6-treated; (b) LT-TMTed with 10% cold deformation and then aged at 200 °C for 80 h

be also observed. The fracture micrograph shows cleavage fracture mechanism with the existence of a great number of cleavage planes together with some tear ridges, the quantity of which is less than that in the T6-treated alloy, as shown in Fig. 6(b). Therefore, such a fracture pattern makes the alloy have lower ductility of about 8%.

Based on the experimental results, a schematic diagram of fracture patterns of the GW61K alloy in T6 and LT-TMT conditions is shown in Fig. 7. Figure 7(a) shows dislocations pile-up at triangular grain boundaries, which leads to crack initiation and propagation along grain boundaries during the deformation of the T6-treated alloy. Figure 7(b) shows the dislocations pile-up at twin boundaries, which leads to crack initiation and propagation along twin boundaries during the deformation of the LT-TMTed alloy. As discussed before, such twins formed during cold tension prior to aging treatment could act as new grains which have high angle grain boundary relationship of about 86° for $\{10\bar{1}2\}\langle 10\bar{1}1\rangle$ twin system. The matrix and the twin boundaries could also hinder the dislocations moving and cause crack initiation and propagation, finally, lead to trans-granular fracture.

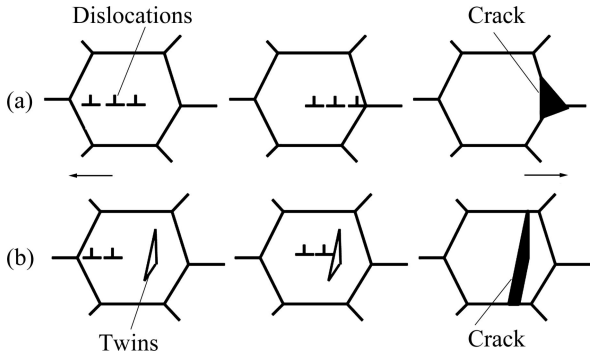

Fig. 7 Sketch of fracture in GW61K alloy: (a) T6 treated; (b) LT-TMTed with 10% cold deformation

In general, such twins could play a role in strengthening the alloys and could also accelerate the fracture of the alloys.

4 Conclusions

1) Dislocation slipping is the dominant deformation mechanism in the alloy during cold tension. Twinning is also attributed to the deformation strain to some extent, which increases with increasing strain.

2) Precipitation kinetics in the deformed alloys is greatly accelerated and the aging time to peak hardness decreases with increasing strain. Cold deformation could also lead to the absence of the early stage for β'' phase decomposition and refine the precipitates of β' phase.

3) The tensile yield strength and ultimate tensile strength increase with the deformation strain in the alloy after LT-TMT, while the elongation decreases. The optimum combination of strength and ductility could be obtained in the alloy after cold deformation with strain of 10% and aging at 200 °C for 36 h. The tensile yield strength, ultimate tensile strength and elongation are 251 MPa, 296 MPa and 8%, respectively.

4) The fracture patterns of the T6-treated and LT-TMTed GW61K alloy exhibit quasi-cleavage and cleavage, respectively.

References

[1] ROKHLIN L L. Magnesium alloys containing rear earth metals [M]. London: Taylor and Francis, 2003: 5−8.

[2] KAMADO S, KOJIMA Y, NINOMIYA R, KUBOTA K. Aging characteristics and high temperature tensile properties of magnesium alloys containing heavy rare earth elements [C]//LORIMER G W. Proceedings of the 3rd International Mg Conference. Manchester, UK: Institute of Materials, 1997: 327−342.

[3] WU Wen-xiang, JIN Li, DONG Jie, ZHANG Zhen-yan, DING Wen-jiang. Research progress of high strength and heat resistant Mg−Gd−Y−Zr alloys [J]. The Chinese Journal of Nonferrous Metals, 2011, 21(11): 2709−2718. (in Chinese)

[4] HU Yao-bo , DENG Juan, ZHAO Chong, WANG Jing-feng, PAN Fu-sheng. Microstructure and mechanical properties of as-quenched Mg−Gd−Zr alloys [J]. Transactions of Nonferrous Metals Society of China, 2011, 21(4): 732−738.

[5] WANG Rong, DONG Jie, FAN Li-kun, ZHANG Ping, DING Wen-jiang. Microstructure and mechanical properties of rolled Mg−12Gd−3Y−0.4Zr alloy sheets [J]. Transactions of Nonferrous Metals Society of China, 2008, 18(s1): s189−s194.

[6] HONMA T, OHKUBO T, HONO K, KAMADO S. Chemistry of nanoscale precipitates in Mg−2.1Gd−0.6Y−0.2Zr (wt.%) alloy investigated by the atom probe technique [J]. Mater Sci Eng A, 2005, 395: 301−306.

[7] HE S M, ZENG X Q, PENG L M, GAO X, NIE J F, DING W J. Precipitation in a Mg−10Gd−3Y−0.4Zr (wt.%) alloy during isothermal ageing at 250 ℃ [J]. J Alloys Compd, 2006, 421: 309−313.

[8] ANTION C, DONNADIEU P, PERRARD F, DESCHAMPS A, TASSIN C, PISCH A. Hardening precipitation in a Mg−4Y−3RE alloy [J]. Acta Mater, 2003, 51: 5335−5348.

[9] NISHIJIMA M, HIRAGA K, YAMASAKI M, KAWAMURA Y. Characterization of β' phase precipitates in an Mg-5 at% Gd alloy aged in a peak hardness condition, studied by high-angle annular detector dark-field scanning transmission electron microscopy [J]. Mater Trans, 2006, 47(8): 2109−2112.

[10] ISMAIL Z H. Microstructure and mechanical properties developed by thermo-mechanical treatment in an Al−Mg−Si alloy [J]. Scripta Metall & Mater, 1995, 32: 457−462.

[11] HILDITCH T, NIE J F, MUDDLE B C. The effect of cold work on precipitation in alloy WE54 [C]// Proceedings of Magnesium Alloys and Their Applications. Wolfsburg, Germany, 1998: 329−334.

[12] JIANG L, JONAS J J, MISHRA R K, LUO A A, SACHDEV A K, GODET S. Twinning and texture development in two Mg alloys subjected to loading along three different strain paths [J]. Acta Mater, 2007, 55: 3899−3910.

[13] MATHIS K, CHMELIK F, JANECEK M, HADZIMA B, TROJANOVA Z, LUKAC P. Investigating deformation processes in

AM60 Mg alloy using the acoustic emission technique [J]. Acta Mater, 2006, 54: 5361−5366.

[14] BARNETT M R. Twinning and the ductility of magnesium alloys: Part II. “Contraction” twins [J]. Mater Sci Eng A, 2007, 464: 8−16.

[15] HE S M, ZENG X Q, PENG L M, GAO X, NIE J F, DING W J. Microstructure and strengthening mechanism of high strength Mg−10Gd−2Y−0.5Zr alloy [J]. J Alloys Compd, 2007, 427: 316−323.

[16] ANTION C, DONNADIEU P, PERRARD F. Hardening precipitation in a Mg−4Y−3RE alloy [J]. Acta Mater, 2003, 51(18): 5335−5348.

[17] NIE J F, MUDDLE B C. Precipitation in magnesium alloy WE54 during isothermal ageing at 250 ℃ [J]. Scripta Mater, 1999, 40(10): 1089−1094.

[18] LU Y Z, WANG Q D, DING W J, ZENG X Q, ZHU Y P. Fracture behavior of AZ91 magnesium alloy [J]. Mater Lett, 2000, 44: 265−268.

低温形变热处理制备 Mg−6Gd−1Y−0.5Zr 合金的力学性能

李德江[1]，曾小勤[1]，谢艳才[1]，吴玉娟[1]，丁文江[1]，陈　彬[2]

1．上海交通大学 材料科学与工程学院 金属基复合材料国家重点实验室，上海 200240；

2．上海交通大学 材料科学与工程学院 分析测试中心，上海 200240

摘　要：对固溶态的 Mg−6Gd−1Y−0.5Zr 合金进行低温形变热处理，处理工艺包括不同应变量的冷拉伸和随后在 200 ℃进行的峰值时效。结果表明：低温形变热处理合金的时效硬化动力学显著加速，随变形量增大，合金的峰值时效时间大幅度缩短。冷拉伸变形量为 10%的合金在 200 ℃峰值时效后的屈服强度、抗拉强度和伸长率分别达到 251 MPa、296 MPa 和 8%，这些性能大大超过传统商业牌号的耐热镁合金 WE54，尽管其总的稀土含量高于 GW61K 合金。

关键词：Mg−Gd−Y−Zr 合金；低温形变热处理；时效硬化；力学性能

(Edited by FANG Jing-hua)